

Tests of Quantum Chromodynamics with the ATLAS experiment

Term Paper "Physics at the LHC"

Alena Lösle

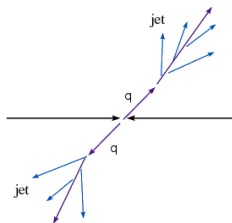
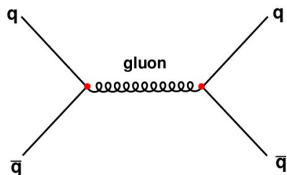
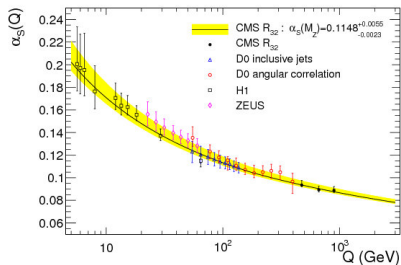
03/07/2014



1. Introduction
2. Jet reconstruction at ATLAS
3. Inclusive jet and dijet cross section measurements
4. W/Z production cross section measurements
5. Production of W+jets
6. Cross section measurements of $t\bar{t}$ production
7. Conclusion and outlook

1.1. Quantum Chromodynamics

- gauge theory of strong interaction described by $SU(3)_C$ symmetry
- couples to colour charge
 - quarks, gluons
- running coupling constant:
 - α_s is energy dependent
 - confinement: no unbound quarks
 - hadronization: formation of particle jets



1.2. Calculation of cross sections

cross section for $AB \rightarrow X$:

$$\sigma_{AB} = \int dx_a dx_b f_{a/A}(x_a, \mu_F^2) f_{b/B}(x_b, \mu_F^2) \hat{\sigma}_{ab}$$

for large momentum scale Q^2 :

calculate $\hat{\sigma}_{ab}$ in perturbation series (pQCD):

$$\hat{\sigma}_{ab} = [\hat{\sigma}_0 + \alpha_s(\mu_R) \hat{\sigma}_1 + \dots]$$

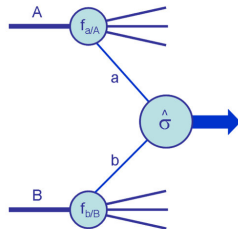
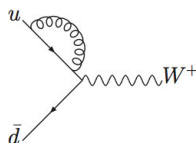
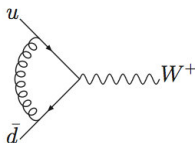
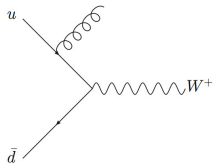
μ_F : factorization scale

μ_R : renormalization scale

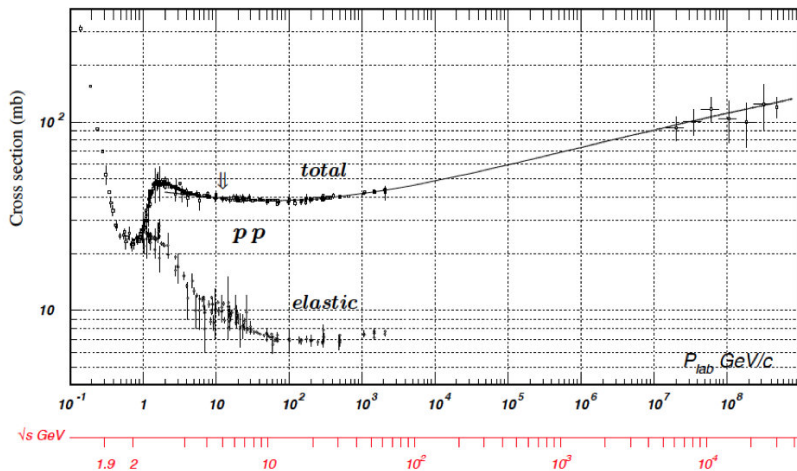
Natural choice for Drell-Yan process:

$$\mu_F = \mu_R = M_Z$$

example for real and virtual corrections at NLO:



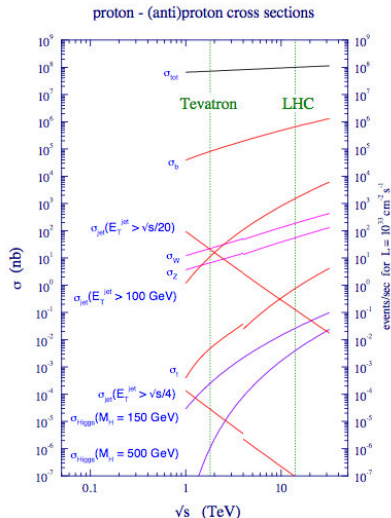
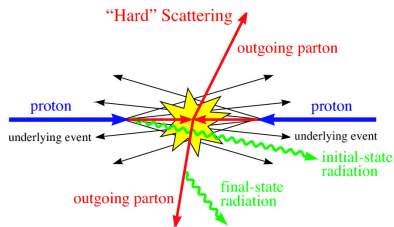
1.3. phenomenology of proton-proton collisions



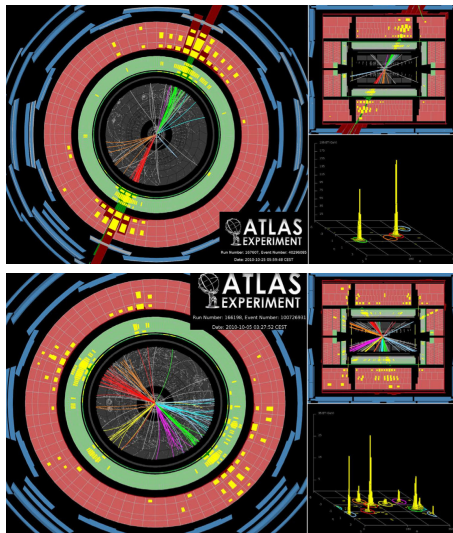
1.3. phenomenology of proton-proton collisions

hard scattering processes:

- high momentum transfer between partons
→ cross section can be calculated in pQCD
- fragmentation of the remaining proton
→ underlying event
- cross section depends on parton distribution functions (PDFs)
→ cannot be described from first principles
→ fit to experimental data



2. Reconstruction of particle jets in ATLAS



quarks and gluons themselves are not observed in the detector
→ jets: collimated spray of energetic hadrons

jet signature in the detector:

- inner detector: particle tracks originating from one primary vertex
- energy deposition in electromagnetic and hadronic calorimeter
- momentum measurement of muons in muon chamber

energy deposition in calorimeter cells are input for jet reconstruction

2.1. The anti- k_T algorithm

requirement: jet definition should be insensitive to collinear and soft gluon radiation
(infrared safety)

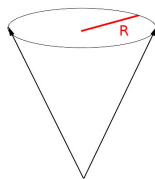
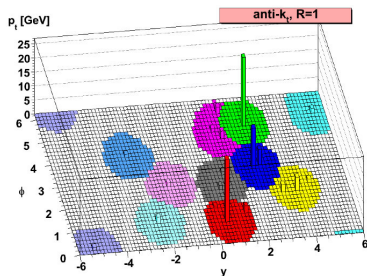
→ anti- k_T algorithm: define jet cone with radius $R = \sqrt{\eta^2 + \Phi^2}$

define distance $d_{ij} = \min\left(\frac{1}{k_{T,i}^2}, \frac{1}{k_{T,j}^2}\right) \frac{\Delta R_{ij}^2}{R^2}$ and $d_{iB} = \frac{1}{k_{T,i}^2}$

- start with energy deposition i and calculate all d_{ij} and d_{iB}

- find minimum distance $\left\{ \begin{array}{l} \text{if min} = d_{i,j} : \text{recombine deposition } i-j \text{ and start again} \\ \text{otherwise: deposition } i \text{ is jet, back to first step} \end{array} \right.$

- stop algorithm when no energy depositions remain



3. Cross section of inclusive jet and dijet measurements

dominant hard scattering process at LHC:
→ tests of QCD, bkg estimation

measurements of double diff. cross section:

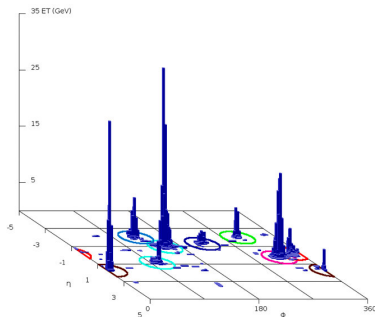
inclusive jet: all jets are considered, $\frac{d^2\sigma}{dp_T dy}$

dijet: only two leading jets are considered

$$\frac{d^2\sigma}{dM dy^*} \text{ with } y^* = \frac{|y_1 - y_2|}{2}$$

jet reconstruction:

- anti- k_T algorithm with $R=0.4$, $R=0.6$
- correction for additional energy (pile-up)
- jet energy scale correction factor (JES): correct for different calorimeter response



3.1. Inclusive jet cross section measurements

event selection:

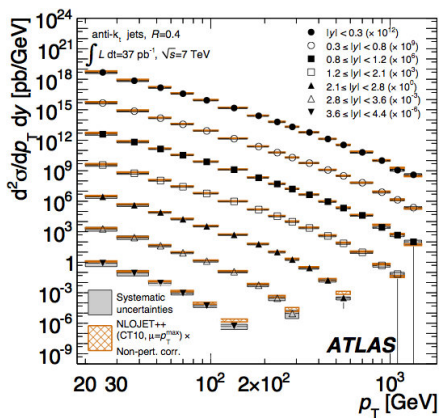
- $p_T^{jet} > 20 \text{ GeV}$, $y < 4.4$
- jets must pass quality selection criteria

unfolding:

signal events are corrected back to particle level taking into account detector acceptance and reconstruction efficiency

theoretical predictions:

fixed-order NLO pQCD calculations with corrections for non-perturbative effects (hadronization, underlying event), no electroweak corrections applied



3.2. Dijet cross section measurements

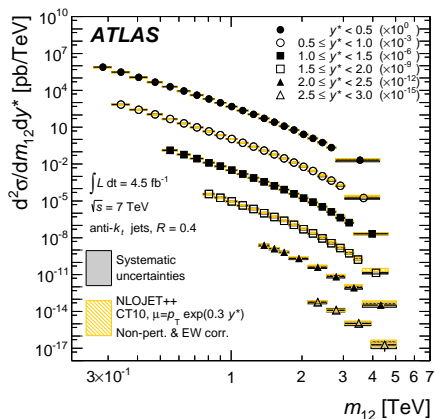
double differential cross section as a function of dijet mass M is sensitive to new resonance
→ beyond SM processes

event selection:

leading (subleading) jets within $y < 3.0$
with $p_T^{lead} > 100$ GeV and $p_T^{sub} > 50$ GeV

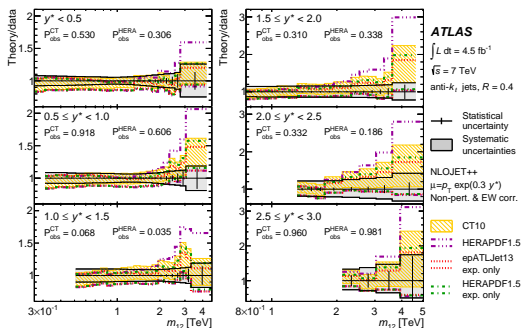
theory predictions:

fixed-order NLO QCD predictions corrected for non-perturbative and electroweak effects



3.2. Dijet cross section measurements

Ratio of the NLO QCD predictions to the measurements of the dijet double-differential cross sections:



dominant exp. syst. uncertainties:

jet energy scale (JES)

($\sim 30 - 60\%$)

jet energy resolution (JER) ($\sim 15\%$
for inclusive, $\sim 8\%$ for dijet)

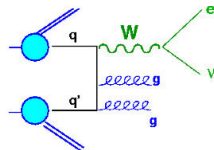
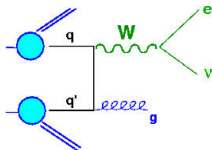
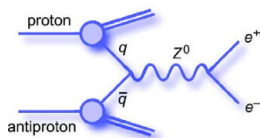
dominant theory uncertainties:

scale variation (missing higher order
terms, PDFs)

comparison of measurements and theory by using a χ^2 -teststatistics
 \rightarrow no major deviation observed

4. W/Z production cross section measurements

W/Z-boson production at hadron colliders:



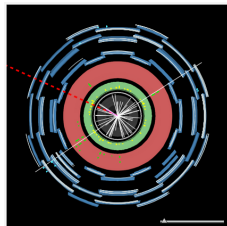
QCD effects contribute only at NLO and beyond
theoretical predictions: NNLO QCD calculations

signal channels: $Z \rightarrow \ell\ell$, $W \rightarrow l\nu$

neutrino only accessible over missing transverse

energy: $E_T^{miss} |_{x,y} = -\sum_i E_{x,y}^i$

$$\rightarrow (E_T^{miss})^2 = (E_x^{miss})^2 + (E_y^{miss})^2$$



4. W/Z production cross section measurements

event selection $W \rightarrow l\nu$

one tight electron/muon, isolated

no additional medium lepton

$$E_T^{miss} > 25 \text{ GeV}$$

$$m_T > 40 \text{ GeV}$$

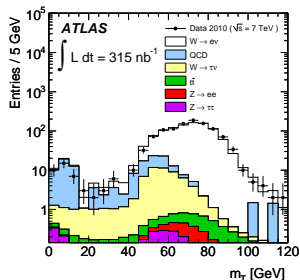
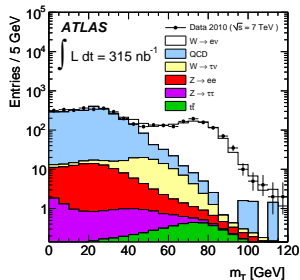
event selection $Z \rightarrow ll$

two medium electrons/muons, isolated

no additional medium lepton

opposite charge, same flavor leptons

$$66 < m_{ll} < 116 \text{ GeV}$$



4. W/Z production cross section measurements

comparison of measurements with theoretical predictions:

$$\sigma_{W/Z}^{\text{tot}} \cdot BR(W/Z \rightarrow l\nu/l\bar{l}) = \frac{N_{W/Z}^{\text{sig}}}{C_{W/Z} \cdot L_{W/Z} \cdot A_{W/Z}}$$

$N_{W/Z}^{\text{sig}}$: number of bkg-subtracted signal events passing selection

$C_{W/Z}$: efficiency for triggering, reconstruction and identification

$L_{W/Z}$: integrated luminosity

$A_{W/Z}$: detector acceptance

	$\sigma_{W(\pm)}^{\text{tot}} \cdot BR(W \rightarrow e\nu)$ [nb]	$\sigma_{W(\pm)}^{\text{tot}} \cdot BR(W \rightarrow \mu\nu)$ [nb]
W^+	$6.27 \pm 0.26(\text{stat}) \pm 0.48(\text{syst}) \pm 0.69(\text{lumi})$	$5.71 \pm 0.23(\text{stat}) \pm 0.30(\text{syst}) \pm 0.63(\text{lumi})$
W^-	$4.23 \pm 0.22(\text{stat}) \pm 0.33(\text{syst}) \pm 0.47(\text{lumi})$	$3.86 \pm 0.20(\text{stat}) \pm 0.20(\text{syst}) \pm 0.42(\text{lumi})$
W	$10.51 \pm 0.34(\text{stat}) \pm 0.81(\text{syst}) \pm 1.16(\text{lumi})$	$9.58 \pm 0.30(\text{stat}) \pm 0.50(\text{syst}) \pm 1.05(\text{lumi})$
	$\sigma_{Z/\gamma^*}^{\text{tot}} \cdot BR(Z/\gamma^* \rightarrow ee)$ [nb], $66 < m_{ee} < 116$ GeV	$\sigma_{Z/\gamma^*}^{\text{tot}} \cdot BR(Z/\gamma^* \rightarrow \mu\mu)$ [nb], $66 < m_{\mu\mu} < 116$ GeV
Z/γ^*	$0.75 \pm 0.09(\text{stat}) \pm 0.08(\text{syst}) \pm 0.08(\text{lumi})$	$0.87 \pm 0.08(\text{stat}) \pm 0.06(\text{syst}) \pm 0.10(\text{lumi})$

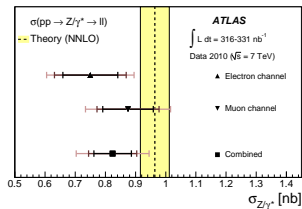
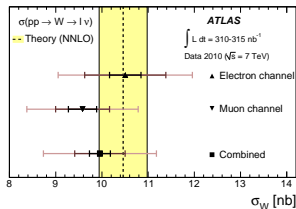
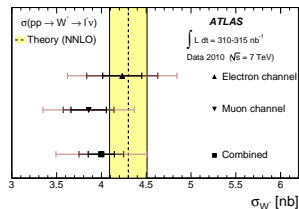
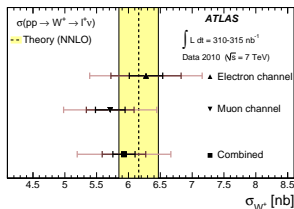
4. W/Z production cross section measurements

systematic uncertainties for electron-channel on total cross section results mainly dominated by $C_{W/Z}$ uncertainties:

Parameter	$\delta C_W/C_W(\%)$	$\delta C_Z/C_Z(\%)$
Trigger efficiency	<0.2	<0.2
Material effects, reconstruction and identification	5.6	8.8
Energy scale and resolution	3.3	1.9
E_T^{miss} scale and resolution	2.0	-
Problematic regions in the calorimeter	1.4	2.7
Pile-up	0.5	0.2
Charge misidentification	0.5	0.5
FSR modelling	0.3	0.3
Theoretical uncertainty (PDFs)	0.3	0.3
Total uncertainty	7.0	9.4

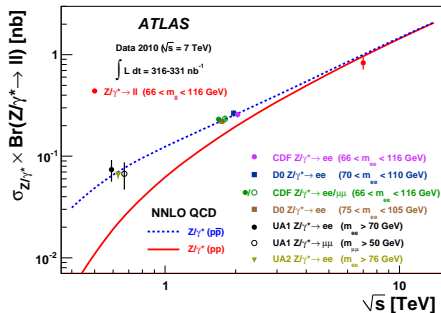
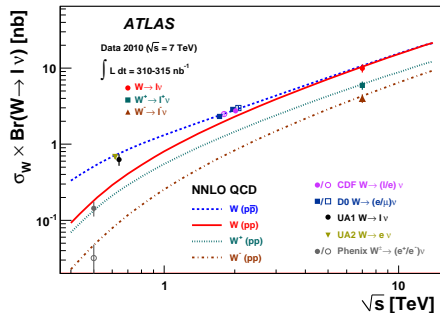
4. W/Z production cross section measurements

Comparison of measurements with NNLO pQCD predictions:
Error bars represent statistical, statistical plus systematic and total uncertainty



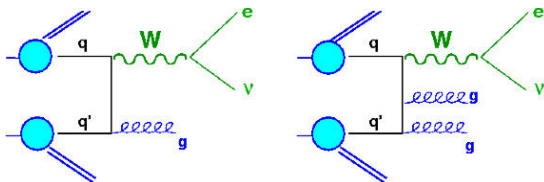
4. W/Z production cross section measurements

Comparison of the combined electron and muon measurements and previous results to theoretical cross section predictions



5. W +jets cross section measurements

measuring the W -production cross section as a function of inclusive jet multiplicity N_{jet}
→ test of pQCD, extract informations about PDFs



Jet selection:

- anti- k_T algorithm with $R=0.4$
- $p_T^{jet} > 30$ GeV
- $|y| < 4.4$ and $\Delta R(l, jet) > 0.5$
- reject jets with $JVF < 0.75$

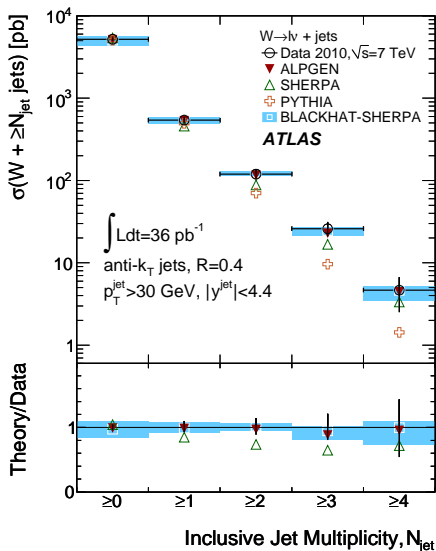
$$JVJF = \frac{\sum p_{T,jet} \text{ tracks from prim. vertex}}{\sum p_{T,jet} \text{ tracks from all vertices}}$$

event selection $W \rightarrow e/\mu\nu$:

same as in previous W -analysis

- $E_T^{miss} > 25$ GeV
- $m_T(W) > 40$ GeV

5. W +jets cross section measurements



theoretical predictions:

NLO QCD calculations corrected for non-perturbative effects

dominant syst. uncertainties:

JES, JER ($\sim 10\%$)

electron identification ($\sim 8\%$)

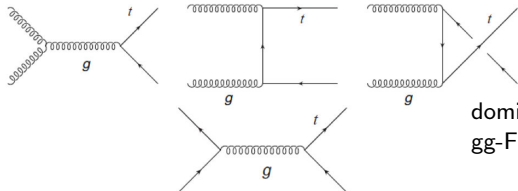
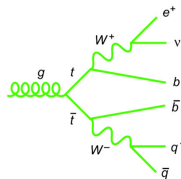
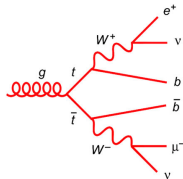
muon momentum resolution ($\sim 6\%$)

luminosity ($\sim 4\%$)

6. $t\bar{t}$ cross section measurements

short recap on top quarks:

- heaviest known particle with $m_t = 173\text{GeV}$
- production of top pair via QCD
- predominant decay channel $t \rightarrow Wb$
- identify b-jets by b-tagging at 70% efficiency



dominant $t\bar{t}$ -production process at LHC:
gg-Fusion (95% at $\sqrt{s} = 14\text{TeV}$)

6. $t\bar{t}$ cross section measurements

single lepton channel:

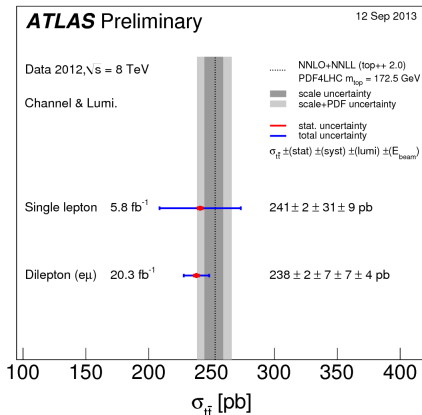
- jet reconstruction with $R=0.4$
- 3 jets with $p_T > 25$ GeV, $|\eta| < 2.5$
- one of these tagged as a b-jet
- $JVF > 0.5$
- tight electron/muon requirements

dilepton channel:

- jet reconstruction with $R=0.4$
- $p_T^j > 25$ GeV, $|\eta| < 2.5$
- one jet tagged as a b-jet
- medium electron/muon requirements
- opposite charge leptons, different flavor

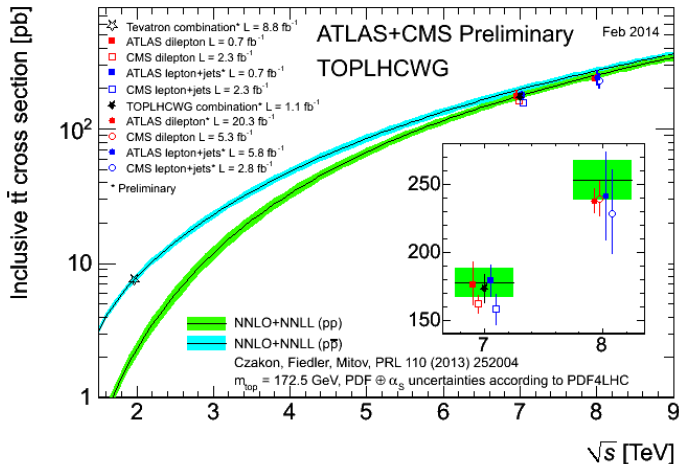
main syst. uncertainties:

- e, μ identification/isolation
- JES, JER, b-tagging, integrated luminosity



6. $t\bar{t}$ cross section measurements

Comparison of the inclusive $t\bar{t}$ cross section measurements and previous results to theoretical predictions:



7. Conclusion and outlook

- cross section measurements presented for inclusive+dijet, W/Z production, W+jets and $t\bar{t}$ production are consistent with (N)NLO QCD predictions
 - test of perturbative QCD
 - measurements provide also information on PDFs
- results are dominated by systematic uncertainties
 - jet energy scale and resolution uncertainties, luminosity uncertainty
- experiments need to reduce uncertainties on jet reconstruction
- further theoretical calculations desirable (NNLO pQCD for inclusive and dijet cross sections)

8. Literature



G. Aad *et al.* [ATLAS Collaboration], Phys. Rev. D **86** (2012) 014022 [arXiv:1112.6297 [hep-ex]].



G. Aad *et al.* [ATLAS Collaboration], arXiv:1312.3524 [hep-ex].



G. Aad *et al.* [ATLAS Collaboration], JHEP **1012** (2010) 060 [arXiv:1010.2130 [hep-ex]].



G. Aad *et al.* [ATLAS Collaboration], Phys. Rev. D **85** (2012) 092002 [arXiv:1201.1276 [hep-ex]].



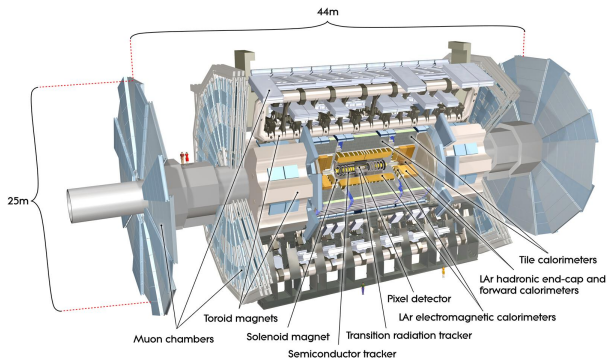
[ATLAS Collaboration], ATLAS-CONF-2012-131.



ATLAS Collaboration], ATLAS-CONF-2013-097.

9. Appendix

The ATLAS detector:



inner detector: silicon pixel and microstrip detectors, TRT detector surrounded by **EM calorimeter:** consists

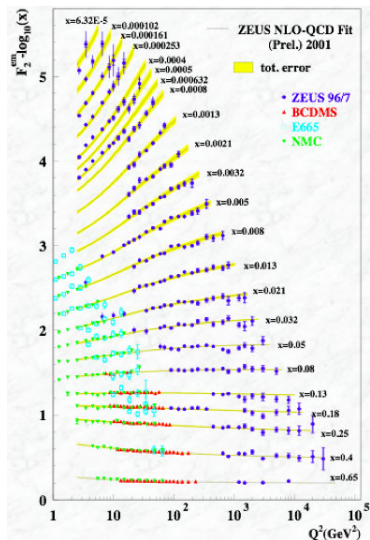
LAr+Pb absorber

hadronic calorimeter: Fe+scintillator with LAr/Cu and LAr/W moduls

muon chamber

9. Appendix

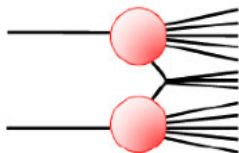
1. Determination of PDFs in DIS



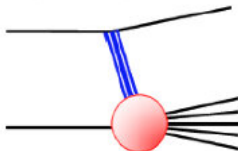
9. Appendix

1. Contributions to total inelastic xsection:

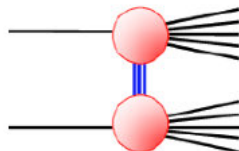
Non-Diffractive
(~34 mb)



Single-Diffractive
(~12 mb)



Double-Diffractive
(~6 mb)



9. Appendix

1. Jet reconstruction: Definition of jet algorithm

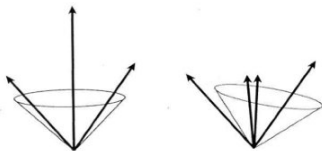


Figure 4.3: *Collinear safety violation. The splitting of one tower into two can change the jet properties.*

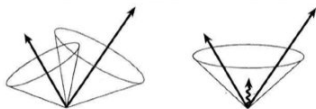
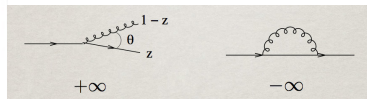
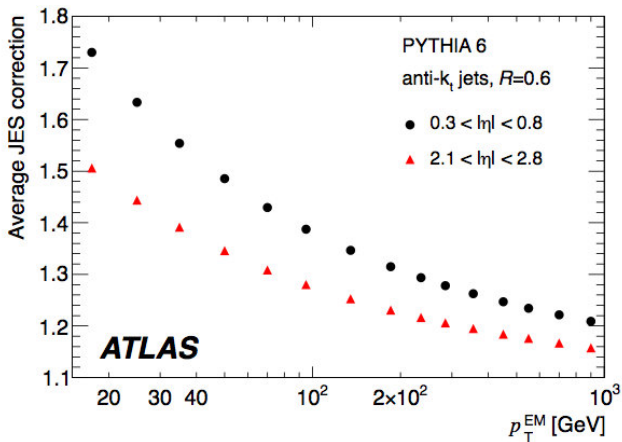


Figure 4.2: *Infrared safety violation: the radiation of a soft gluon can change the jet properties.*



9. Appendix

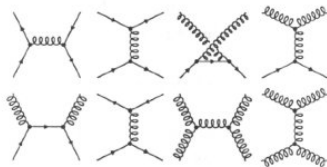
2. Jet energy correction factor



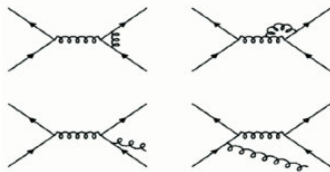
9. Appendix

3.1. Jet production mechanism at hadron colliders:

Often many diagrams contribute:



Higher order corrections important:



9. Appendix

3.3. Systematic uncertainties inclusive and dijet dominant systematic uncertainties on inclusive jet cross section measurements:

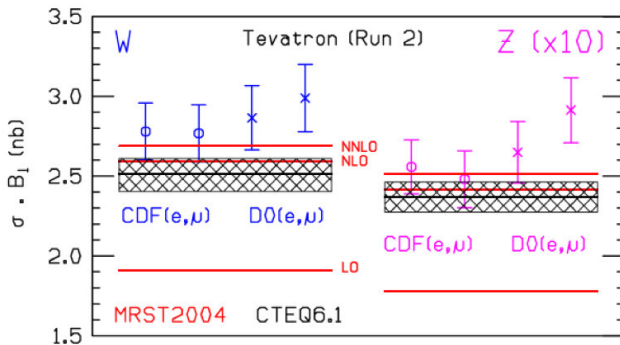
p_T [GeV]	$ y $	JES	JER	Trigger	Jet Rec.
20–30	2.1–2.8	$+35\%$ -30%	17%	1%	2%
20–30	3.6–4.4	$+65\%$ -50%	13%	1%	2%
80–110	< 0.3	10%	1%	1%	1%

dominant systematic uncertainties on dijet cross section measurements:

m_{12} [TeV]	y^*	JES	JER	Trigger	Jet Rec.
0.37–0.44	2.0–2.5	$+46\%$ -27%	7%	1%	2%
2.55–3.04	4.0–4.4	$+110\%$ -50%	8%	2%	2%
0.21–0.26	< 0.5	10%	1%	1%	2%

9. Appendix

4. W/Z production NNLO predictions



9. Appendix

4. W/Z production cross section systematic uncertainties

	W^+				W^-				W			
	Electron channel											
	value	stat	syst	lumi	value	stat	syst	lumi	value	stat	syst	lumi
N_W^{sig}	604.2	25.2	7.6	2.0	403.2	20.8	7.5	1.5	1007.5	32.7	10.8	3.5
$L_W [\text{nb}^{-1}]$	315	-	-	35	315	-	-	35	315	-	-	35
C_W	0.656	-	0.046	-	0.662	-	0.046	-	0.659	-	0.046	-
A_W	0.466	-	0.014	-	0.457	-	0.014	-	0.462	-	0.014	-
	Muon channel											
	value	stat	syst	lumi	value	stat	syst	lumi	value	stat	syst	lumi
N_W^{sig}	655.6	26.6	6.2	4.7	425.0	21.7	5.4	3.9	1080.6	34.4	11.2	8.5
$L_W [\text{nb}^{-1}]$	310	-	-	34	310	-	-	34	310	-	-	34
C_W	0.765	-	0.031	-	0.748	-	0.030	-	0.758	-	0.030	-
A_W	0.484	-	0.015	-	0.475	-	0.014	-	0.480	-	0.014	-

main bkg contributions:

- $W \rightarrow \tau\nu$: leptonic τ decay
- $Z \rightarrow ll$: $z \rightarrow \mu\mu$ with one missing muon contributes to W-analysis
- $Z \rightarrow \tau\tau$: single or double leptonic tau decay
- $t\bar{t}$ production
- QCD processes: semileptonic decays of heavy quarks, hadrons misidentified als electrons and electrons from conversions

9. Appendix

4. W/Z production cross section systematic uncertainties on C_W in muon channel:

Parameter	$\delta C_W/C_W(\%)$	$\delta C_Z/C_Z(\%)$
Trigger efficiency	1.9	0.7
Reconstruction efficiency	2.5	5.0
Momentum scale	1.2	0.5
Momentum resolution	0.2	0.5
E_T^{miss} scale and resolution	2.0	-
Isolation efficiency	1.0	2.0
Theoretical uncertainty (PDFs)	0.3	0.3
Total uncertainty	4.0	5.5

9. Appendix

W/Z production cross section measurements, fiducial cross section:

$$\sigma_{W/Z}^{fid} \cdot BR(W/Z \rightarrow l\nu/l\bar{l}) = \sigma_{W/Z}^{tot} \cdot BR(W/Z \rightarrow l\nu/l\bar{l}) \cdot A_{W/Z}$$

$A_{W/Z}$: detector acceptance for considered W/Z-boson decay

	$\sigma_{W(\pm)}^{tot} \cdot BR(W \rightarrow e\nu)$ [nb]	$\sigma_{W(\pm)}^{tot} \cdot BR(W \rightarrow \mu\nu)$ [nb]
W^+	$6.27 \pm 0.26(\text{stat}) \pm 0.48(\text{syst}) \pm 0.69(\text{lumi})$	$5.71 \pm 0.23(\text{stat}) \pm 0.30(\text{syst}) \pm 0.63(\text{lumi})$
W^-	$4.23 \pm 0.22(\text{stat}) \pm 0.33(\text{syst}) \pm 0.47(\text{lumi})$	$3.86 \pm 0.20(\text{stat}) \pm 0.20(\text{syst}) \pm 0.42(\text{lumi})$
W	$10.51 \pm 0.34(\text{stat}) \pm 0.81(\text{syst}) \pm 1.16(\text{lumi})$	$9.58 \pm 0.30(\text{stat}) \pm 0.50(\text{syst}) \pm 1.05(\text{lumi})$
	$\sigma_{Z/\gamma^*}^{tot} \cdot BR(Z/\gamma^* \rightarrow ee)$ [nb], $66 < m_{ee} < 116$ GeV	$\sigma_{Z/\gamma^*}^{tot} \cdot BR(Z/\gamma^* \rightarrow \mu\mu)$ [nb], $66 < m_{\mu\mu} < 116$ GeV
Z/γ^*	$0.75 \pm 0.09(\text{stat}) \pm 0.08(\text{syst}) \pm 0.08(\text{lumi})$	$0.87 \pm 0.08(\text{stat}) \pm 0.06(\text{syst}) \pm 0.10(\text{lumi})$

	$\sigma_{W(\pm)}^{fid} \cdot BR(W \rightarrow e\nu)$ [nb]	$\sigma_{W(\pm)}^{fid} \cdot BR(W \rightarrow \mu\nu)$ [nb]
W^+	$2.92 \pm 0.12(\text{stat}) \pm 0.21(\text{syst}) \pm 0.32(\text{lumi})$	$2.77 \pm 0.11(\text{stat}) \pm 0.12(\text{syst}) \pm 0.30(\text{lumi})$
W^-	$1.93 \pm 0.10(\text{stat}) \pm 0.14(\text{syst}) \pm 0.21(\text{lumi})$	$1.83 \pm 0.09(\text{stat}) \pm 0.08(\text{syst}) \pm 0.20(\text{lumi})$
W	$4.85 \pm 0.16(\text{stat}) \pm 0.34(\text{syst}) \pm 0.53(\text{lumi})$	$4.60 \pm 0.15(\text{stat}) \pm 0.20(\text{syst}) \pm 0.51(\text{lumi})$
	$\sigma_{Z/\gamma^*}^{fid} \cdot BR(Z/\gamma^* \rightarrow ee)$ [nb], $66 < m_{ee} < 116$ GeV	$\sigma_{Z/\gamma^*}^{fid} \cdot BR(Z/\gamma^* \rightarrow \mu\mu)$ [nb], $66 < m_{\mu\mu} < 116$ GeV
Z/γ^*	$0.33 \pm 0.04(\text{stat}) \pm 0.03(\text{syst}) \pm 0.04(\text{lumi})$	$0.43 \pm 0.04(\text{stat}) \pm 0.02(\text{syst}) \pm 0.05(\text{lumi})$

4. W/Z production cross section measurements

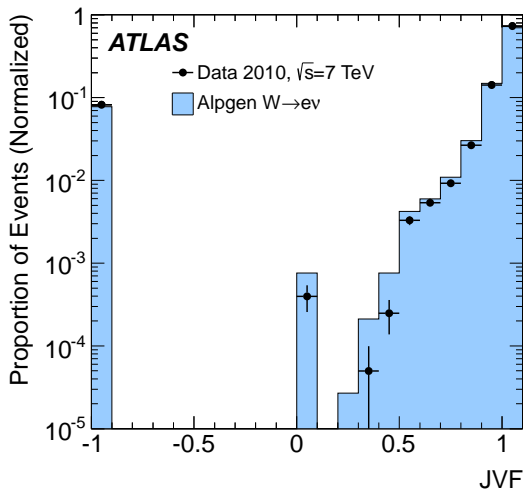
all systematic uncertainties on total cross section results mainly dominated by $C_{W/Z}$ uncertainties:

	W^+				W^-				W			
Electron channel												
	value	stat	syst	lumi	value	stat	syst	lumi	value	stat	syst	lumi
N_W^{sig}	604.2	25.2	7.6	2.0	403.2	20.8	7.5	1.5	1007.5	32.7	10.8	3.5
$L_W [\text{nb}^{-1}]$	315	-	-	35	315	-	-	35	315	-	-	35
C_W	0.656	-	0.046	-	0.662	-	0.046	-	0.659	-	0.046	-
A_W	0.466	-	0.014	-	0.457	-	0.014	-	0.462	-	0.014	-
Muon channel												
	value	stat	syst	lumi	value	stat	syst	lumi	value	stat	syst	lumi
N_W^{sig}	655.6	26.6	6.2	4.7	425.0	21.7	5.4	3.9	1080.6	34.4	11.2	8.5
$L_W [\text{nb}^{-1}]$	310	-	-	34	310	-	-	34	310	-	-	34
C_W	0.765	-	0.031	-	0.748	-	0.030	-	0.758	-	0.030	-
A_W	0.484	-	0.015	-	0.475	-	0.014	-	0.480	-	0.014	-

9. Appendix

4. W+jets cross section measurements

JVF distribution:



9. Appendix

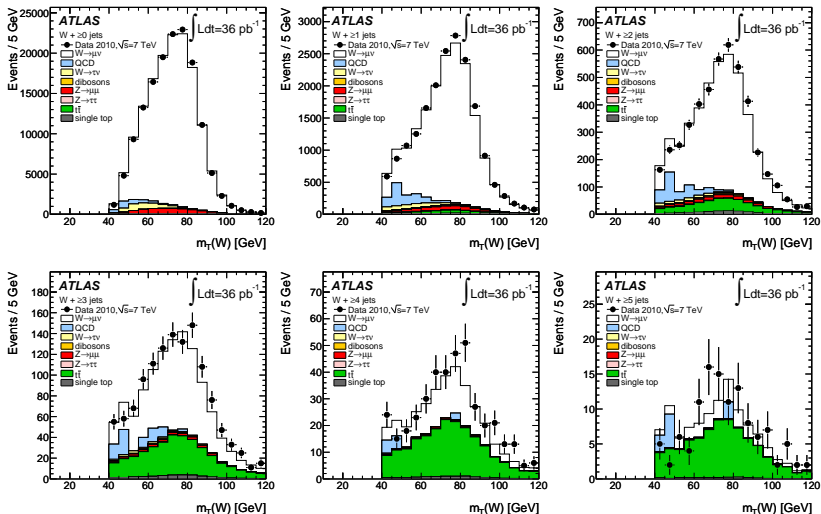
5. W +jets cross section measurements systematic uncertainties for electron and muon final states:

$W \rightarrow e\nu$ channel			
Effect	Range	Cross Section Uncertainty (%)	
		$N_{\text{jet}} \geq 1$	$N_{\text{jet}} \geq 4$
Jet and cluster energy scales	2.5–14% (dependent on jet η and p_T)	+9.0, –6.6	+37, –35
Jet energy resolution	$\sim 10\%$ on each jet (dependent on jet η and p_T)	± 1.6	± 6
Electron trigger	$\pm 0.5\%$	+0.6, –0.5	± 1
Electron reconstruction	$\pm 1.5\%$	+1.7, –1.6	± 4
Electron identification	± 2 –8% (dependent on electron η and p_T)	+4.3, –4.0	+10, –9
Electron energy scale	± 0.3 –1.6% (dependent on η and p_T)	± 0.6	+1, –3
Electron energy resolution	$< 0.6\%$ of the energy	± 0.0	< 1
Pile-up removal requirement	$\sim 1.5\%$ in lowest jet p_T bin	± 1.1	± 3
Multijet QCD background shape	from template variation	± 0.7	± 11
Unfolding	ALPGEN vs. SHERPA	± 1.5	± 6
Luminosity	$\pm 3.4\%$	+3.8, –3.6	+9, –8
NNLO cross section for W/Z	$\pm 5\%$	± 0.2	< 1
NLO cross section for $t\bar{t}$	$^{+7}_{-10}\%$	± 0.3	± 10
Simulated $t\bar{t}$ shape	from samples with more or less ISR	± 0.1	+12, –21

$W \rightarrow \mu\nu$ channel			
Effect	Range	Cross Section Uncertainty (%)	
		$N_{\text{jet}} \geq 1$	$N_{\text{jet}} \geq 4$
Jet and cluster energy scales	2.5–14% (dependent on jet η and p_T)	+8.2, –6.2	+33, –26
Jet energy resolution	10% on each jet (dependent on jet η and p_T)	± 1.5	± 5
Muon trigger	$\pm 0.7\%$ ($\pm 0.6\%$ in barrel (endcap))	± 0.6	± 1
Muon reconstruction and identification	$\pm 1.1\%$	± 1.1	± 2
Muon momentum scale	$\pm 0.4\%$	+0.2, –0.3	< 1
Muon momentum resolution	$\pm 6\%$	± 0.1	< 1
Pile-up removal requirement	$\sim 1.5\%$ in lowest jet p_T bin	± 1.0	± 3
Multijet QCD background shape	from template variation	+0.8	–20
Unfolding	ALPGEN vs. SHERPA	± 0.2	< 1
Luminosity	$\pm 3.4\%$	+3.7, –3.5	± 7
NNLO cross section for W/Z	$\pm 5\%$	± 0.4	< 1
NLO cross section for $t\bar{t}$	$^{+7}_{-10}\%$	+0.4, –0.3	+10, –7
Simulated $t\bar{t}$ shape	from samples with more or less ISR	< 0.1	+13, –15

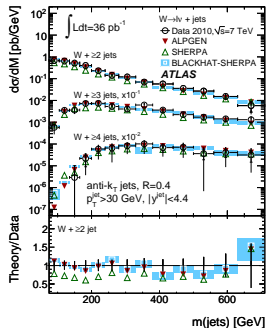
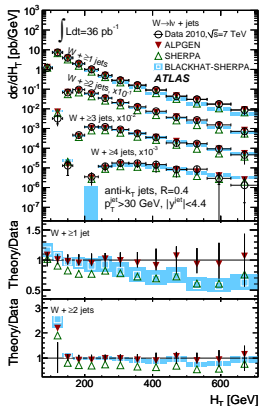
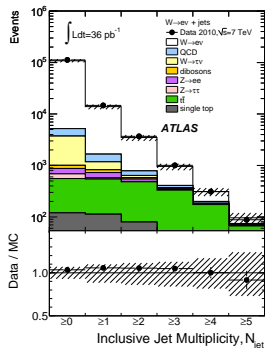
9. Appendix

5. W +jets cross section measurements transv. mass distributions for different jet multiplicities:



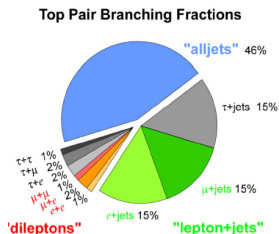
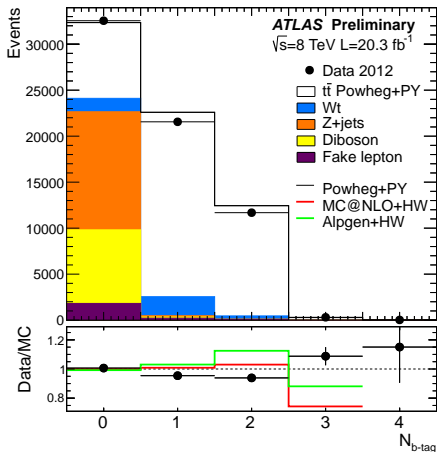
9. Appendix

5. W+jets cross section measurements



9. Appendix

6. $t\bar{t}$ cross section measurements distribution of the number of b-tagged jets:



9. Appendix

6. $t\bar{t}$ cross section measurements

systematic uncertainties dilepton:

Uncertainty	$\Delta\epsilon_{e\mu}/\epsilon_{e\mu}$ (%)	$\Delta C_b/C_b$ (%)	$\Delta\sigma_{t\bar{t}}/\sigma_{t\bar{t}}$ (%)	$\Delta\sigma_{t\bar{t}}$ (pb)	$\Delta\epsilon_s/\epsilon_s$ (%)
Data statistics	-	-	0.72	1.7	0.57
$t\bar{t}$ modelling	0.91	-0.61	1.52	3.6	0.61
Initial/final state radiation	-0.76	0.26	1.23	2.9	0.37
Parton density functions	1.08	-	1.09	2.6	0.06
QCD scale choices	0.30	-	0.30	0.7	0.00
Single-top modelling	-	-	0.38	0.9	0.56
Single-top/ $t\bar{t}$ interference	-	-	0.15	0.4	0.25
Single-top Wt cross-section	-	-	0.70	1.7	0.24
Diboson modelling	-	-	0.42	1.0	0.19
Diboson cross-sections	-	-	0.03	0.1	0.01
Z+jets extrapolation	-	-	0.05	0.1	0.02
Electron energy scale/resolution	0.43	0.01	0.48	1.1	0.03
Electron identification/isolation	1.28	0.00	1.42	3.4	0.05
Muon momentum scale/resolution	0.01	0.01	0.05	0.1	0.02
Muon identification/isolation	0.50	0.00	0.52	1.2	0.01
Lepton trigger	0.15	0.00	0.16	0.4	0.01
Jet energy scale	0.46	0.07	0.49	1.2	0.11
Jet energy resolution	-0.44	0.04	0.59	1.4	0.08
Jet reconstruction/vertex fraction	0.02	0.01	0.04	0.1	0.01
b -tagging	-	0.13	0.42	1.0	0.09
Pileup modelling	-0.30	0.05	0.28	0.7	0.05
Misidentified leptons	-	-	0.38	0.9	0.12
Total systematic	2.29	0.69	3.12	7.4	1.02
Integrated luminosity	-	-	3.11	7.4	0.11
LHC beam energy	-	-	1.70	4.0	0.00
Total uncertainty	2.29	0.69	4.77	11.3	1.17

systematic uncertainties single lepton:

Source	$e+ \geq 3 \text{ jets}$	$\mu+ \geq 3 \text{ jets}$	combined
Jet/MET reconstruction, calibration	6.7, -6.3	5.4, -4.6	5.9, -5.2
Lepton trigger, identification and reconstruction	2.4, -2.7	4.7, -4.2	2.7, -2.8
Background normalization and composition	1.9, -2.2	1.6, -1.5	1.8, -1.9
b -tagging efficiency	1.7, -1.3	1.9, -1.1	1.8, -1.2
MC modelling of the signal	± 12	± 11	± 11
Total	± 14	± 13	± 13